Title

Mechanism of docosahexaenoic acid-induced inhibition of in vitro Aβ1–42 fibrillation and Aβ1–42-induced toxicity in SH-S5Y5 cells

Author(s)

Shahdat Hossain, Michio Hashimoto, Masanori Katakura, Koji Miwa, Toshio Shimada, Osamu Shido

Journal

Journal of Neurochemistry, Volume111, Issue2

Published

October 2009

URL

https://doi.org/10.1111/j.1471-4159.2009.06336.x

J N C 6 3 3 6 B
Journal Name Manuscript No.
Dispatch: 25.8.09 Journal: JNC CE: Shuail
Author Received: No. of pages: 12 PE: Raymond
JOURNAL OF NEUROCHEMISTRY | 2009 doi: 10.1111/j.1471-4159.2009.06336.x

Mechanism of docosahexaenoic acid-induced inhibition of *in vitro* $A\beta_{1-42}$ fibrillation and $A\beta_{1-42}$-induced toxicity in SH-S5Y5 cells

Shahdat Hossain,*† Michio Hashimoto,* Masanori Katakura,* Koji Miwa,* Toshio Shimada T.‡ and Osamu Shido*

*Department of Environmental Physiology, Shimane University Faculty of Medicine, Izumo, Japan
†Department of Biochemistry & Molecular Biology, Jahangirnagar University, Savar, Dhaka, Bangladesh
‡Department of Internal Medicine, Shimane University Faulty of Medicine, Izumo, Shimane, Japan

Abstract

The mechanism of the effect of docosahexaenoic acid (DHA; C22:6, *n*-3), one of the essential brain nutrients, on *in vitro* fibrillation of amyloid β ($A\beta_{1-42}$), $A\beta_{1-42}$-oligomers and its toxicity imparted to SH-SY5Y cells was studied with the use of thioflavin T fluorospectroscopy, laser confocal microfluorescence, and transmission electron microscopy. The results clearly indicated that DHA inhibited $A\beta_{1-42}$-fibrill formation with a concomitant reduction in the levels of soluble $A\beta_{1-42}$ oligomers. The polymerization (into fibrils) of preformed oligomers treated with DHA was inhibited, indicating that DHA not only obstructs their formation but also inhibits their transformation into fibrils. sodium dodecyl sulfate–polyacrylamide gel electrophoresis (12.5%), Tris–Tricine gradient(4–20%) gel electrophoresis and western blot analyses revealed that DHA inhibited at least 2 species of $A\beta_{1-42}$ oligomers of 15–20 kDa, indicating that it hinders these on-pathway tri/tetrameric intermediates during fibrillation. DHA also reduced the levels of dityrosine and tyrosine intrinsic fluorescence intensity, indicating DHA interrupts the microenvironment of tyrosine in the $A\beta_{1-42}$ backbone. Furthermore, DHA protected the tyrosine from acrylamide collisional quenching, as indicated by decreases in Stern–Volmer constants. 3-[4,5-Dimethylthiazol-2-yl]-2,5-diphenyltetrazolium bromide-reduction efficiency and immunohistochemical examination suggested that DHA inhibits $A\beta_{1-42}$-induced toxicity in SH-SY5Y cells. Taken together, these data suggest that by restraining $A\beta_{1-42}$ toxic tri/tetrameric oligomers, DHA may limit amyloidogenic neurodegenerative diseases, Alzheimer's disease.

Keywords: $A\beta_{1-42}$ oligomer, $A\beta_{1-42}$ peptide, docosahexaenoic acid, fibrillation, SH-S5Y5 cells, toxicity.
J. Neurochem. (2009) 10.1111/j.1471-4159.2009.06336.x

Alzheimer's disease (AD) is characterized by anomalous self-assembled deposits of amyloid β (Aβ) peptides in the neuritic plaques and neurofibrillar tangles of the AD brain (Selkoe 1991). $A\beta_{1-42}$ is the major amyloid component in the neuritic plaques of the affected brain (Iwatsubo *et al.* 1994), indicating a key role of $A\beta_{1-42}$ in amyloidogenesis and the associated neurobehavioral impairments in AD (Berman *et al.* 2008). The mechanism of fibrillation and the mechanistic association of fibers with AD pathology are still far from clear, although numerous studies have been done on the topic. Depending on various factors, including peptide length (Jarrett *et al.* 1993), concentration (Burdick *et al.* 1992), and pH (Fraser *et al.* 1991) of the solvent, $A\beta_{1-42}$ passes through diverse stages, including α-helix to β-sheet transformation, nucleation, beading or elongation of oligomers (fibrillation) and coalescence of fibrils into larger aggregates (Serpell 2000). These molecular transitions are typically associated with neuronal loss and cognitive deficits in AD. Therefore, the foremost strategy for preventing AD is to inhibit amyloid deposition.

The major objectives of this study are to evaluate the effect and mechanism of docosahexaenoic acid (DHA) on *in vitro* $A\beta_{1-42}$ fibrillation. Although DHA, one of the predominant and essential *n*-3 polyunsaturated fatty acids in brain lipids,

Received March 30, 2009; revised manuscript received August 10, 2009; accepted August 11, 2009.

Address correspondence and reprint requests to Michio Hashimoto, Department of Environmental Physiology, Shimane University Faculty of Medicine, Izumo 693-8501, Japan.
E-mail: michio1@med.shimane-u.ac.jp

Abbreviations used: AD, Alzheimer's disease; Aβ, amyloid β; DHA, docosahexaenoic acid; DT, dityrosine; LT, lag time; MTT, 3-[4,5-dimethylthiazol-2-yl]-2,5-diphenyltetrazolium bromide; SDS, sodium dodecyl sulfate; TEM, transmission electron microscopy; ThT, thioflavin T.

reduces the level of $A\beta_{1-40}$ in the cortex of $A\beta_{1-40}$-infused AD model rats (Hashimoto *et al.* 2005a) and mice (Lim *et al.*2005) with concurrent protection (Hashimoto *et al.* 2002) and prevention (Hashimoto *et al.* 2005b) of cognitive deficits in these animals, the mechanism of the anti-amyloidogenic properties of DHA is not clearly understood. The more hydrophobic $A\beta_{1-42}$ is not only more copious than $A\beta_{1-40}$ in the AD brain (Iwatsubo *et al.* 1994), but its fibrillation kinetics is also very different from that of the $A\beta_{1-40}$ (Bitan *et al.* 2003). Therefore, we investigated the mechanism of the effect of DHA on the *in vitro* fibrillation of $A\beta_{1-42}$ and on Aβ toxicity imparted to SH-SY5Y cells. The present interest in $A\beta_{1-42}$ stems largely from the fact that numerous human trials are ongoing to determine whether DHA is effective in the treatment and/or delaying the symptoms of AD (Morris *et al.* 2003) associated with DHA deficiency (Söderberg *et al.* 1991; Prasad *et al.* 1998). Most importantly, while substantial evidence indicates that insoluble Aβ deposits are associated with AD pathology, recent evidence suggests that soluble Aβ oligomers, more than matured fibrils, correlate strongly with neuronal dysfunction, damage and AD symptoms (Haass and Selko 2007). With this in mind, we investigated the effect of DHA on the levels of soluble $A\beta_{1-42}$ oligomers and examined whether the $A\beta_{1-42}$ fibrillogenesis imparts toxicity to SH-SY5Y cells and whether it could be inhibited by DHA treatment. Our results demonstrated that DHA significantly reduces $A\beta_{1-42}$ fibrillation and *in vitro* toxicity. Therefore, DHA could be viewed as an excellent therapeutic agent against $A\beta_{1-42}$-induced neurodegenerative diseases, including AD.

Materials and methods

Materials

Amyloid β-protein ($A\beta_{1-42}$) was purchased from the Peptide Institute Inc. (Osaka, Japan); thioflavin T (ThT) was purchased from Sigma-Aldrich (St Louis, MO, USA); rabbit anti-human Aβ [N] antibody (code #18584), conformation-specific anti-oligomer antibody (A11) (unconjugated form), and mouse anti-tubulin antibody (Tuj1) were purchased from Biosource International, Inc. (CA, USA). Anti-dityrosine (DT) monoclonal antibody was purchased from Japan Institute for the Control of Aging (Shizuoka, Japan). All other chemicals were of analytical grade.

Amyloid β 1–42 peptide preparation for analysis of aggregation

Amyloid β 1–42 peptide was dissolved in 1,1,1,3,3,3-hexafluoro-2-propanol at a concentration of 500 μM to produce uniform, non-aggregated Aβ and immediately stored at −80°C after N_2 bath until use. On the day of use, the 1,1,1,3,3,3-hexafluoro-2-propanol-dissolved amyloid was spun down to eliminate pre-fibrillar amyloids, if any, and then blown with N_2 gas at ice-cold temperatures and re-dissolved in the assembly buffer for aggregation studies. If necessary the peptide mixture was instantly filtered through Centricut Eppendorf tubes (Kurabo, Osaka, Japan) of a molecular mass limit of 10 kDa to exclude pre-fibrillar materials.

Preparation of docosahexaenoic acid

Docosahexaenoic acid (50 mg) dissolved in 200 μL ethanol (Cayman Chemical Company, MI, USA) was stored (in 5.0-μL aliquots) at −80°C until use. The aliquot was directly suspended in ultra pure water and used at desired concentration containing 0.002% ethanol. Only freshly prepared DHA was used.

Dose-dependent effect of docosahexaenoic acid on $A\beta_{1-42}$ *in vitro* fibrillation

Fibrillation was carried out as previously described (Hashimoto *et al.* 2008) with some modifications. $A\beta_{1-42}$ peptide (50 μM) was suspended in the desired volume of assembly buffer (100 μL of 50 mM Tris–HCl buffer, pH 7.4, containing 100 mM NaCl and 0.01% sodium azide) with or without DHA. The final concentrations of DHA were 5, 10, and 20 μM. The reaction mixture was taken into oil-free PCR tubes flushed with nitrogen gas to obviate any effect of atmospheric oxygen, and incubated at 37°C for 24 h. The incubation was stopped by placing the tubes on ice.

Thioflavin T fluorescence assay of $A\beta_{1-42}$

After 24 h of incubation at 37°C, 40-μL aliquots from each tube were gently removed and mixed with 210 μL of 5 μM ThT in 50 mM glycine–NaOH buffer, pH 8.5, and subjected to fluorescence spectroscopy (Hitachi F-2500 fluorescence spectrophotometer) at excitation (λ_{ex}) and emission (λ_{em}) wavelengths of 448 and 487 nm, respectively.

Effects of docosahexaenoic acid on the kinetics of $A\beta_{1-42}$ fibrillation

The effect of 20 μM of DHA on the kinetics of $A\beta_{1-42}$ fibrillation was evaluated by using 5, 10, and 50 μM of $A\beta_{1-42}$. Briefly, the reaction mixture containing 1.0 mL of 50 mM Tris–HCl buffer, pH 7.4, 100 mM NaCl, 0.01% sodium azide, and the desired amount of $A\beta_{1-42}$ with or without DHA was taken into Eppendorf tubes and incubated at 37°C. At desired time intervals, a 40-μL of the peptide mixture was gently removed and added to 210 μL of 5 μM ThT for fluorescence assay.

Microfluorescence study

A 2.5-μL aliquot of the fibrillated $A\beta_{1-42}$ peptide (50 μM) sample from the ThT-$A\beta_{1-42}$ assay with (20 μM) or without DHA was diluted 2× with 5 μM ThT in 50 mM glycine–NaOH buffer, pH 8.5, transferred onto slides and photographed by the confocal laser microscope system (CLSM FV300; Olympus, Tokyo, Japan). The images were converted to color histograms by ImageJ, which generates the RGB values automatically. The mean values were averaged from three slides for each group.

Transmission electron microscopy

After completion of $A\beta_{1-42}$ fibrillation for 24 h at 37°C with or without DHA, an aliquot was used for electron microscopy. In brief, a 4-μL sample was placed on a copper grid and stained with 1% uranyl acetate; excess uranyl acetate was then removed from the grid with distilled water, air dried and examined under a Hitachi H-7000

transmission electron microscope (TEM) with an operating voltage of 75 kV.

$A\beta_{1-42}$ oligomer formation and destabilization assay

The inhibitory effects of DHA on oligomer formation (assay A) and destabilization (assay B) were evaluated. In assay A, $A\beta_{1-42}$ fibrillation (50 μM) was carried out in the presence (5, 10, and 20 μM) or absence of DHA at 37°C for 24 h, centrifuged at 13 800 *g* for 30 min at 4°C to separate the supernatant fraction containing the soluble oligomers, and the content of $A\beta_{1-42}$ in the supernatant fraction was then quantified by the $A\beta_{1-42}$-specific antibody (primary anti-human Aβ [N] antibody) by ELISA, as described below. The level of $A\beta_{1-42}$ was calibrated by using standard $A\beta_{1-42}$ solutions.

In assay B, $A\beta_{1-42}$ fibrillation (50 μM) was initially conducted in the absence of DHA; soluble oligomers were then separated as described for assay A, and the supernatant fraction was treated with (5, 10, and 20 μM DHA) or without DHA for 24 h at 37°C. This method facilitated DHA interaction directly with the oligomers. The oligomers were then incubated at 37°C for 24 h for fibrillation, and the level of oligomer was determined by the oligomer-specific antibody, as previously described (Hashimoto *et al.* 2008). Sister samples prepared at parallel settings were subjected to ThT fluorescence assay.

ELISA

Briefly, ELISA plates were coated with oligomer fractions (with 0.1 M sodium bicarbonate, pH 9.6, as a coating buffer) by incubation at 4°C overnight and then blocked with 3% (assay A) or 10% (assay B) bovine serum albumin containing Tris-buffered saline containing 0.3% Triton X-100. The primary antibody (anti-human Aβ [N] antibody that detects the N-terminal sequence Gly-Val-Val-Ile-Ala in assay A, and oligomer-specific antibody (Glabe 2004; Kayed *et al.* 2003) in assay B, at 1 : 1000 dilution was incubated in the plate for 1 h at 37°C. Horseradish peroxidase-coupled anti-rabbit IgG (Biosource International, Inc.) was used as the secondary antibody. Tetramethylbenzidine was used as a substrate to develop color. Wells coated with only 0.1 M sodium bicarbonate, pH 9.6, and/or monomeric $A\beta_{1-40}$ were used as negative controls. Color was measured with a multiwell plate reader at 450 nm.

Gel electrophoresis

The $A\beta_{1-42}$ oligomer preparations with or without DHA were subjected to 10% sodium dodecyl sulfate (SDS)–polyacrylamide gel electrophoresis and/or 4–20% Tris–Tricine gradient gel at 60 V for 4 h. The monomeric amyloids were run in parallel. Proteins of known molecular weight were used as size standards (Bio-Rad, Hercules, CA, USA). The bands were stained with Coomassie brilliant blue and visualized with Molecular Imager FX (Bio-Rad) and/or transferred to a polyvinylidene difluoride membrane. The membrane was probed with the primary anti-human Aβ [N] antibody (code #18584) overnight at 4°C and with anti-rabbit IgG conjugated with horseradish peroxidase (1 : 3000) for 1 h and then processed for the detection of chemiluminescence according to the manufacturer's instructions for densitometry (enhanced chemiluminescence plus western blotting detection system; Amersham, GE Health Care).

Dityrosine assay

The formation of DT was initially confirmed by scanning the fluorescence emission of fibrillated samples (50 μM of $A\beta_{1-42}$) at λ_{ex} of 300 nm and λ_{em} of 350–520 nm (Atwood *et al.* 2004). The levels of DT were then quantitatively measured by ELISA as described previously (Kato *et al.* 1998). Briefly, 50 μL of the (50 μM)$A\beta_{1-42}$ fibrillated samples with or without DHA, were mixed with coating buffer (0.1 M sodium bicarbonate, pH 9.6) and left overnight at 4°C. The primary monoclonal (1 : 500) and secondary antibodies were anti-DT (code MDT-020p) and peroxidase-labeled anti-mouse IgG antibody, respectively. Color was developed with appropriate substrate, and absorbance was measured at 450 nm.

Tyrosine 10 intrinsic fluorescence spectroscopy

Tyrosine emission scans were conducted with the λ_{ex} set to 277 nm, and the λ_{em} varied from 285 to 345 nm. Spectra were normalized to their maximum intensity. Tyr10 emission intensity of the respective samples with or without DHA was measured at λ_{em} of 304 nm. A cuvette with a 3 mm path-length was used.

Tyrosine 10 fluorescence quenching of $A\beta_{1-42}$ fibrils by acrylamide

Steady state fluorescence quenching of Tyr10 was measured as previously described (Padrick and Miranker 2001). Aliquots (0.5 μL) of the stock quencher solution were added to the cuvette containing 40 μL of 50 μM $A\beta_{1-42}$ fiber with or without DHA in 210 μL of 50 mM Tris–HCl buffer, pH 7.4, containing 100 mM of NaCl and 0.01% sodium azide. To compare the Tyr10 quenching of the unfolded-$A\beta_{1-42}$, an equal volume of $A\beta_{1-42}$ fiber (50 μM) was defibrillated (reconverted) into the soluble monomeric form by incubating it with 0.1 N NaOH at 80°C for 2 h. Fluorescence quenching data were analyzed by the general form of the Stern–Volmer equation:

$$F_o/F = 1 + K_{SV}[Q],$$

where F_o and F are the fluorescence intensities in the presence and the absence of quencher $[Q]$ and K_{sv} is the Stern–Volmer quenching constant. The value of K_{sv} is of interest because it reflects the collisional frequency of Tyr10-fluorophore with acrylamide and, hence, the extent to which the Tyr10 residues are shielded from such collisions by the surrounding matrix.

Toxicity assay of $A\beta_{1-42}$

The cytotoxic effect of $A\beta_{1-42}$ fibrillation was assessed by 3-[4,5-dimethylthiazol-2-yl]-2,5-diphenyltetrazolium bromide (MTT) reduction assay. Briefly, SH-SY5Y cells were plated at a density of 1×10^4 cells/well in 96-well plates. Fibrillation was conducted with $A\beta_{1-42}$ at final concentrations of 0, 0.5, 1.0, 2.0, 5.0, and 10 μM, with (5 μM) or without DHA ($A\beta_{1-42}$ alone) for 48 h under serum-free conditions. The medium was then replaced with OPTI-MEM serum-free medium. MTT was added and the plate was incubated at 37°C for 4 h. The MTT solution was removed, dimethylsulfoxide (100 μL) was added, the plate was shaken for a few minutes and read at 550 nm. In parallel sets of experiments, the medium was collected, centrifuged for 20 min at 13 400 *g*, and the pellets were resuspended and prepared for ThT assay and TEM grids.

Immunostaining and confocal microscopy for $A\beta_{1-42}$ fibers in the cell culture and cell morphology

The post-fixed (by 4% *p*-formaldehyde) cells were washed, blocked with 3% goat serum in TBS containing 0.3% Triton X-100 for 1 h, and incubated with the primary antibody [rabbit anti-human Aβ [N] antibody and mouse anti-neuron-specific class III β-tubulin antibody (Tuj1)] at 4°C overnight. The cells were then washed and incubated for 1 h with the secondary antibody [anti-rabbit/mouse IgG conjugated Alexa 488-conjugated secondary antibody (1 : 5000; Invitrogen Corp., Carlsbad, CA, USA)]. The nuclei were stained with propidium iodide (2.0 μg/mL) for 30 min. Fluorescence was visualized by confocal laser microscope (CLSM FV300; Olympus) and processed by Adobe Photoshop (Adobe Systems, Mountain View, CA, USA).

Statistical analyses

Results are expressed as means ± SEM. Data were analyzed by Student's *t*-test or one-way ANOVA followed by Fisher's PLSD for *post hoc* comparisons. Kinetic data of nucleation-independent and nucleation-dependent fibrillation were subjected to non-linear one-phase exponential association equation and variable-slope sigmoidal equation, respectively. The Stern–Volmer plot was fitted to simple regression analyses. The statistical programs used were StatView® 4.01 (Abacus Concepts, Inc., Berkeley, CA, USA) and GraphPad prism (version 4.00; GraphPad Software Inc., San Diego, CA, USA). A level of $p < 0.05$ was considered statistically significant.

Results

Effect of docosahexaenoic acid on *in vitro* fibrillation of $A\beta_{1-42}$

Although 5 μM of DHA had no significant effect on $A\beta_{1-42}$ fibrillation, 10 and 20 μM significantly decreased fibril formation by 32% and 41%, respectively, compared with that of the control (Fig. 1a). After examining the inhibitory effect of the three concentrations on the $A\beta_{1-42}$ fibrillogenesis at the end point, we studied the effect of DHA on the kinetics of fibrillogenesis to obtain a better temporal resolution. Fibril formation increased as a function with the concentration of $A\beta_{1-42}$ peptide (Fig. 1b). Depending on the concentration of peptide, we observed both nucleation-dependent and -independent fibrillation of $A\beta_{1-42}$. Fibrillation at 50 μM of $A\beta_{1-42}$ concentration did not exhibit any lag time (LT); instead, an exponential growth phase was prominent after a short period of time lag (< 10 min), indicating its strong fibrillation potential at higher amyloid concentrations. The data obtained from 50 μM of $A\beta_{1-42}$ fibrillation were thus best fitted to the one-phase exponential association equation. The rate constant of nucleation-independent fibrillation significantly decreased (by 30%) in the presence of 20 μM of DHA [50 μM of $A\beta_{1-42}$ vs. 50 μM of $A\beta_{1-42}$ + DHA: 1.2 ± 0.1/h: 0.75 ± 0.04/h with a corresponding half-life (T_{50}): 0.58 and 0.93 h, respectively] (Fig. 1c). Indeed, the fibrillogenesis at 5 and 10 μM of $A\beta_{1-42}$ concentrations started typically from a lag phase, to an exponential growth phase and then, to a plateau phase (Fig. 1d). The kinetics at lower concentrations appeared as a characteristic sigmoid curve. Here, we also calculated the LT and T_{50} by fitting the data to a variable-slope sigmoidal equation. The LT reflects the capacity of DHA to delay the nucleation phase of the fibrillation process. At 95% confidence interval, half-life was increased by DHA (T_{50}: 10 μM of $A\beta_{1-42}$ vs. 10 μM of $A\beta_{1-42}$ + DHA = 18.9 ± 0.07 vs.23.1 ± 0.09 h; 5 μM of $A\beta_{1-42}$ vs. 5 μM of $A\beta_{1-42}$ + DHA = 22.2 ± 0.05 vs.25.0 ± 0.07 h, with a corresponding LT of 15.9, 19.8, 18.9 and 21.9.1 h, respectively). DHA lengthened the time both at the lag phase and during the growth of fibrillation for 3–4 h.

Effect of docosahexaenoic acid on microfluorescence of $A\beta_{1-42}$ aggregates

Amyloid β 1–42 aggregates showed characteristic green fluorescence after their binding with thioflavinT (Fig. 2a and b). The $A\beta_{1-42}$ 50 + 20 μM of DHA samples had a lower number of green fluorescent areas than did the $A\beta_{1-42}$ controls. The green fluorescent areas were transformed into (semi)quantitative data by image analyzer (ImageJ). The fluorescence intensity of the green illuminated areas was significantly lower (> 75%) in the DHA-treated samples than that in the controls (Fig. 2c), suggesting that the fibrillation of $A\beta_{1-42}$ was inhibited by DHA.

Effect of docosahexaenoic acid on the $A\beta_{1-42}$ morphology

The control samples ($A\beta_{1-42}$ alone) contained abundantly aggregated amyloid fibrils in the assembly buffer, whereas the $A\beta_{1-42}$ + DHA samples contained only very small amounts. The former fibrils exhibited typical morphology with beaded structures leading to necklace-like decorative filaments and an extensive branching morphology (Fig. 2d–f). They were 18 ± 1.25 nm in diameter, with a twisting helical pattern, and some demonstrated projections emerging from the body (Fig. 2e and f). Flat ribbon and round-shaped fibrils as single or intertwined strands were also observed (Fig. 2g). The lengths of the fibers differed from grid to grid and were almost inconspicuous because of the presence of extensive branching. Their average length (from branching point to branching point) was 100–2000 nm. The fibers of the $A\beta_{1-42}$ + DHA samples (Fig. 2h and i) were narrower (diameter 6–7 nm) and shorter (90–160 nm) than those of the control. The electron microscopy grids of $A\beta_{1-42}$ + DHA samples had numerous amorphous aggregates showing a congested form (Fig. 2j and k). These results indicate that DHA obstructs the fibrillogenesis of $A\beta_{1-42}$.

Effect of docosahexaenoic acid on $A\beta_{1-42}$ oligomer levels

Examination of the concentration-dependent inhibition efficiency of DHA on oligomer formation and destabilization revealed that oligomer formation was significantly inhibited in the presence of DHA, as indicated by the decrease in the anti-$A\beta_{1-42}$ antibody-determined $A\beta_{1-42}$ content in the

LOW RESOLUTION FIG

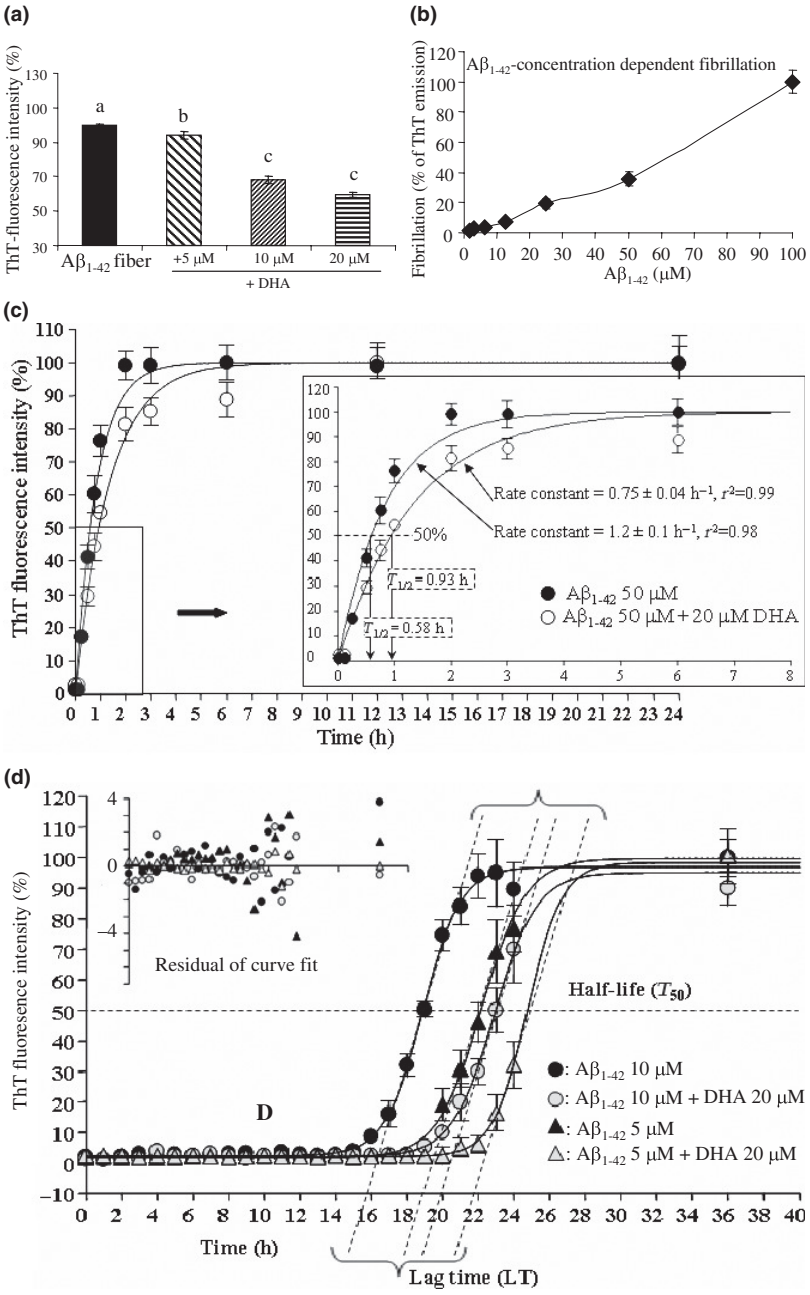

Fig. 1 (a) DHA dose-dependently reduced thioflavin T (ThT) fluorescence intensity, demonstrating its anti-$A\beta_{1-42}$-fibrillation (50 μM) properties [bars with different superscript letters ($^{a-c}$) are significantly different at $p < 0.05$ (one-way ANOVA)]. (b) $A\beta_{1-42}$ peptide fibrillation increased with the concentration (0–100 μM) of the amyloid (ThT-emission was normalized to that of the 100 μM amyloid fiber). (c) Nucleation-independent fibrillation for $A\beta_{1-42}$ was observed at 50 μM of $A\beta_{1-42}$ concentration. The initial lag phase was < 10 min, followed by a rapid exponential growth phase (~6–7 h), thereafter it reached a plateau. The emission data acquired for the first 10 min were excluded from the calculation. The rate constant was significantly higher for 50 μM of $A\beta_{1-42}$ than that for the $A\beta_{1-42}$ + 20 μM of DHA. (d): Nucleation-dependent fibrillation kinetics of $A\beta_{1-42}$ fibrillation. T_{50} represents the time required to achieve 50% ThT fluorescence intensity. LT represents the lag time, defined as the intercept between the slopes of the curve and the axis of incubation time. Inset is the residuals of curve fit (for details see Materials and methods).

soluble fraction of $A\beta_{1-42}$ + DHA samples (Fig. 3a). DHA also significantly destabilized ($p < 0.05$) the preformed oligomers, as indicated by the reduced (by > 12%) levels of oligomer-specific antibody-determined oligomers (Fig. 3b). Furthermore, the ThT-emission intensities were lower in the preformed $A\beta_{1-42}$ oligomers incubated with DHA (data not shown).

Effect of docosahexaenoic acid on the $A\beta_{1-42}$ oligomer size

Sodium dodecyl sulfate–polyacrylamide gel electrophoresis analyses of the soluble oligomers revealed two bands of molecular mass ~15–20 kDa (equivalent to tri/tetramer of $A\beta_{1-42}$) in the $A\beta_{1-42}$ samples (Fig. 3c, lane 2, bands iii and iv). In the $A\beta_{1-42}$ + DHA samples, the average density of the bands (~15–20 kDa) of three independent experiments was significantly reduced (Fig. 3c, upper panel). Also, the soluble oligomers were subjected to non-reducing Tris–Tricine gradient (4–20%) gel (Fig. 3d). The density of the oligomeric band (in between 15 and 20 kDa) was again statistically reduced ($p < 0.05$) with DHA treatment (Fig. 3d upper panel). The presence of these discrete $A\beta_{1-42}$ oligomers was further confirmed by western blot

LOW RESOLUTION COLOUR FIG

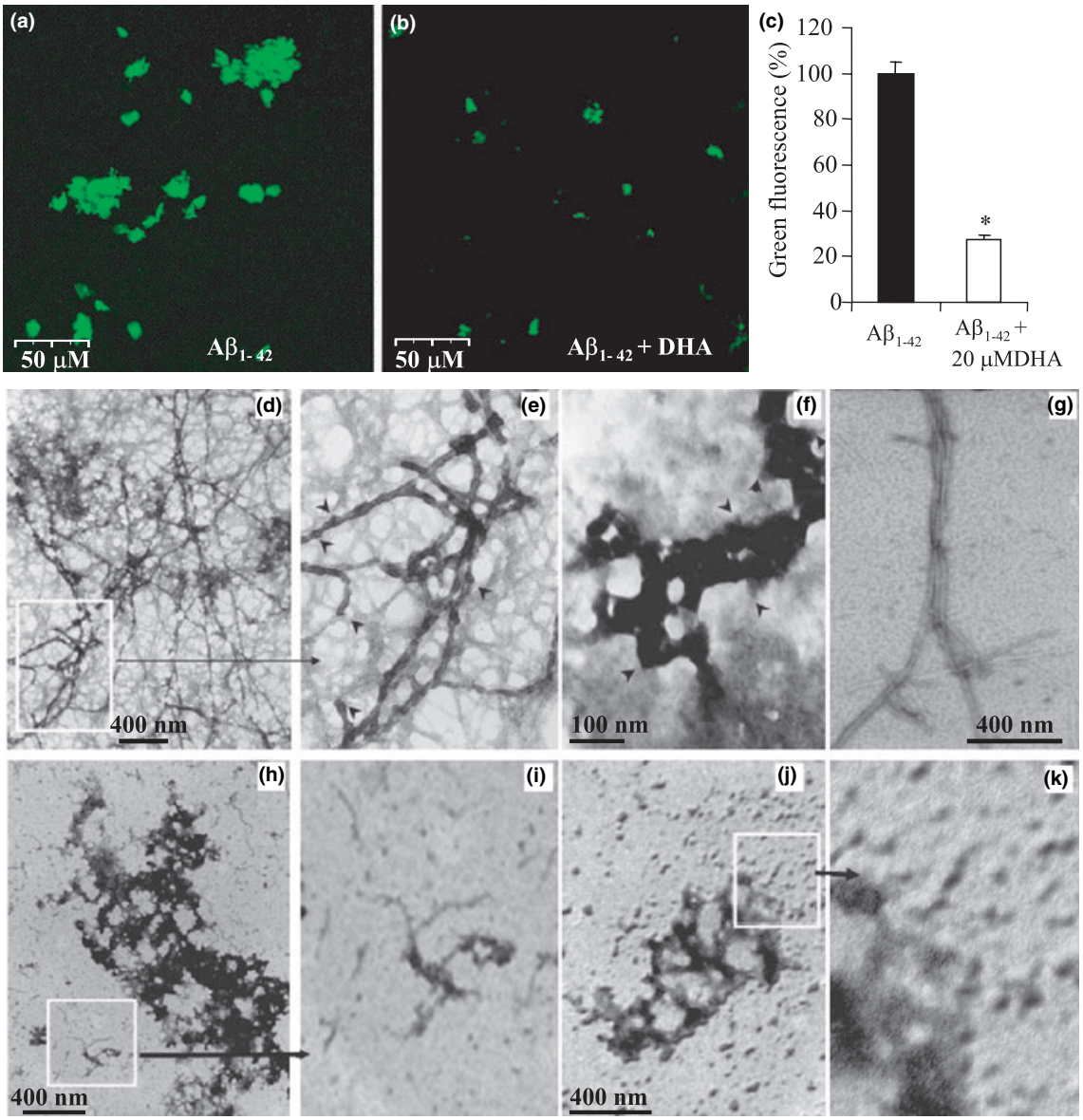

Fig. 2 Thioflavin T staining of polymerized amyloid aggregates, which under fluorescence illumination appear green. (a) $A\beta_{1-42}$ (50 μM) controls. (b) $A\beta_{1-42}$ (50 μM) + 20 μM of DHA (c) The microfluorescence signals, as digitized to histogram data by using ImageJ, were significantly (*$p < 0.05$) lower in the DHA samples. (d–k) Transmission electron micrographs of the $A\beta_{1-42}$ fibrils in the absence (d–g) or presence (h–k) of DHA. The control samples had both beaded (d, e, and f) chains and ribbons or round-shaped (g) fibrils with a twisting helical morphology and branching. Some of the beaded fibrils had projections arising from the body (arrowheads) (f). The typical morphology of $A\beta_{1-42}$ fibrils collapsed in the presence of DHA. Some of the grids of the $A\beta_{1-42}$ + DHA samples had single-stranded narrow fragments with diffused and unstructured fibrils (h and i), and the amyloids appeared mostly as amorphous structures or globs (j and k) across the entire viewable areas.

analyses. The 15–20 kDa oligomers were again visualized (Fig. 3e) and the intensity of these oligomers was reduced with DHA treatment (Fig. 3f). To confirm SDS resistance, the preformed $A\beta_{1-42}$ fibrils were incubated with 0.02% SDS for a further 24 h. The presence of β-sheets was authenticated by ThT-emission peak at 487 nm and is clearly indicative of the resistance to solvation by SDS; the inhibitory effect of DHA on SDS-resistant fibrils still remained significant (data not shown).

Effect of docosahexaenoic acid on Tyr10 intrinsic fluorescence properties and dityrosine levels

Fibrillation of $A\beta_{1-42}$ was accompanied by a decrease of about 20–30% in the intrinsic fluorescence intensity of

LOW RESOLUTION FIG

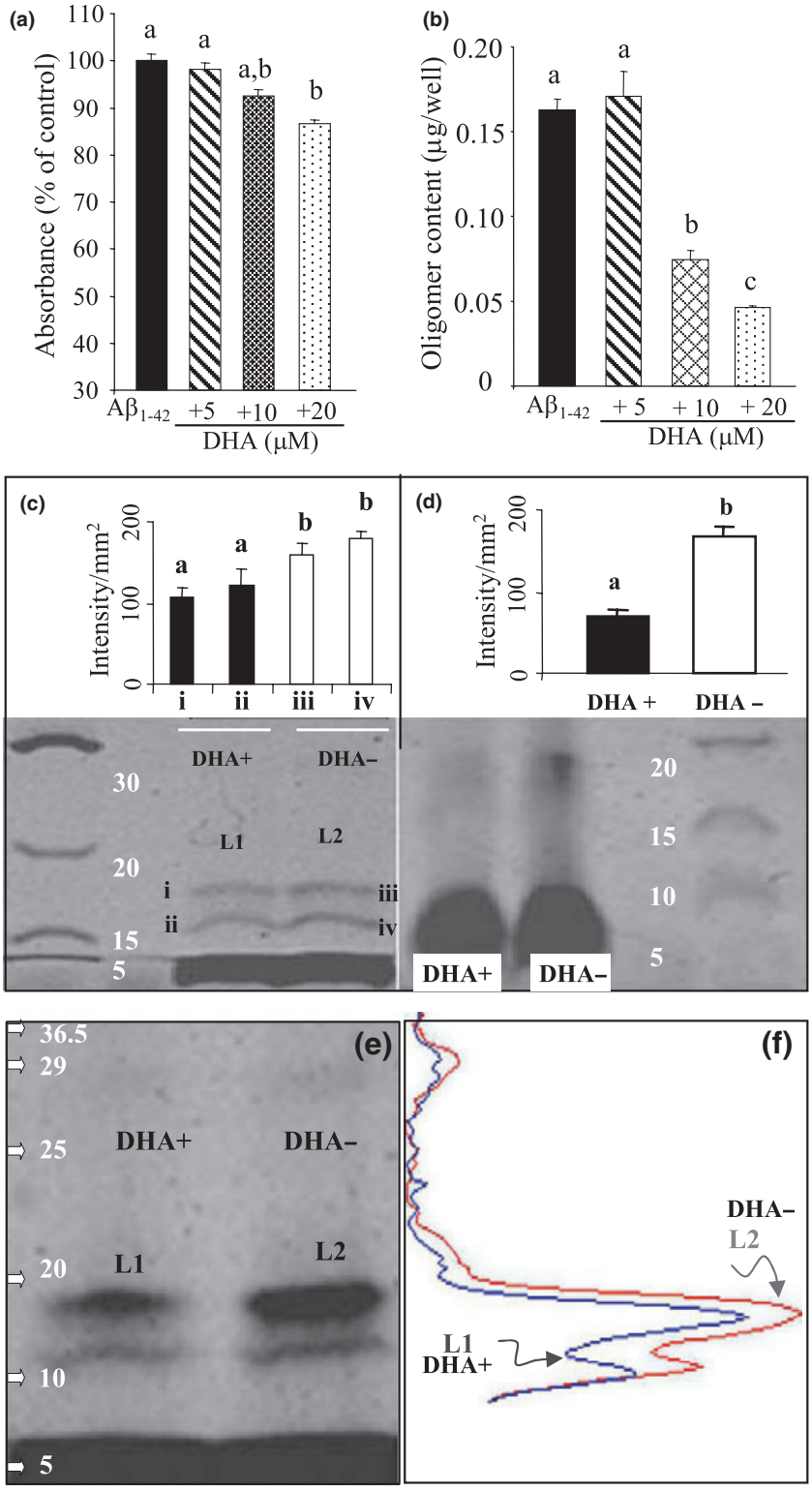

Fig. 3 Inhibitory effect of DHA on the formation (a) and destabilization (b) of $A\beta_{1-42}$ oligomers. (Lower panels of c, d, and e) Representative figures of the effect of DHA on the $A\beta_{1-42}$ oligomer size by gel electrophoresis. The soluble oligomer fractions was applied directly to SDS (12.5%) (c) and 4–20% Tris–Tricine gradient (d) gel analyses. The bands were stained with Coomassie brilliant blue. Two major amyloid species of molecular mass ~15 and ~20 kDa (equivalent to tri-tetramers) were found in both gels. The decreased density of these bands (upper panels of c and d) in the $A\beta_{1-42}$ + DHA samples, when compared with those of the $A\beta_{1-42}$, clearly indicates the inhibitory effect of DHA on the tri-to tetrameric (~15–20 kDa) oligomers. The sizes of these oligomeric bands were further confirmed by western blot (e), where the density (f) also was reduced with DHA treatment. Bars (a, b, c, and d) with different superscript letters ($^{a-c}$) are significantly different at $p < 0.05$ (one-way ANOVA).

Tyr10, when compared with that in the unfolded fresh monomeric $A\beta_{1-42}$. Interestingly, the intrinsic intensity of Tyr10 reverted (by ~30%) to that of the monomeric form when the $A\beta_{1-42}$ fibrils were re-transformed (by solubilizing the matured fibrils in 0.1 N NaOH) into the monomeric form, indicating that 'shield-in' and 'expose-out' of Tyr10 ensued during the process of fibrillation. DHA further decreased Tyr10 intrinsic fluorescence intensity, although no shift of the

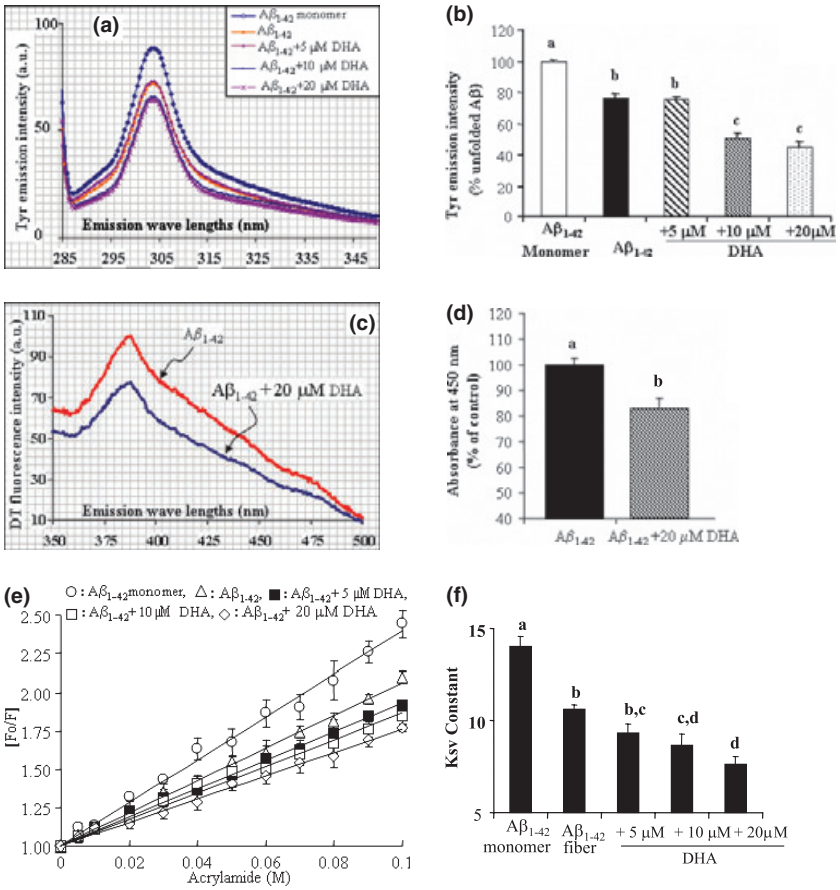

Fig. 4 The effect of DHA on the intrinsic tyrosine (Tyr10) fluorescence properties of $A\beta_{1-42}$. (a) Intrinsic fluorescence measurements of $A\beta_{1-42}$ (50 μM) were carried out at λ_{ex} maximum of 277 nm and emission was collected between 280 and 330 nm. The λ_{em} maximum of Tyr10 was 304 nm. (b) The emission intensity decreased in the $A\beta_{1-42}$ fibrils, when compared with that of the unfolded non-aggregated monomeric $A\beta_{1-42}$. Tyr10 emission intensity further decreased with the increasing concentrations of DHA. (c) The fluorescence spectra of dityrosine (DT) was recorded at λ_{ex} = 300 nm and λ_{em} = 350–500 nm. (d) The levels of DT in the sister samples were then measured by ELISA using anti-DT antibody. (e) Stern–Volmer analysis of the quenching of $A\beta_{1-42}$ fluorescence by acrylamide. Each symbol shown is the average of three measurements. All lines extrapolate back to $b = 1(\pm 0.025)$ at $[Q] = 0$ M. R^2 for fits of acrylamide quenching are 0.992, 0.995, 0.995, 0.989, and 0.994, respectively, for unfolded-$A\beta_{1-42}$ monomers, $A\beta_{1-42}$ fibrils alone, $A\beta_{1-42}$ + 5 μM of DHA, $A\beta_{1-42}$ + 10 μM of DHA, and $A\beta_{1-42}$ + 20 μM of DHA, respectively. (f) Values of K_{sv} for quenching of tyrosine fluorescence by acrylamide. Bars (a, b, c, and d) with different superscript letters ($^{a-d}$) are significantly different at $p < 0.05$ (one-way ANOVA).

emission maximum (λ_{emmax}) occurred. The inhibitory effect was significant at 10 and 20 μM of DHA (Fig. 4a and b). $A\beta_{1-42}$ fibrillation was also accompanied by an increased level of DT; however, the level of DT decreased significantly in the $A\beta_{1-40}$ + 20 μM of DHA samples (Fig. 4c and d). To obtain the state of Tyr10 solvent accessibility in $A\beta_{1-42}$, Tyr10 fluorescence intensity was then measured in the presence of a neutral quencher, acrylamide. Tyr10 emission quenching data analyzed by the Stern–Volmer plot were linear (mono-phasic) in both the presence and the absence of DHA (Fig. 4e). The Stern–Volmer constant (K_{sv}) that determines the degree of solvent exposure of Tyr10 decreased significantly with the higher concentrations of DHA (Fig. 4f).

Effect of docosahexaenoic acid on $A\beta_{1-42}$-induced toxicity

SH-SY5Y cells exhibited the highest MTT-redox activity in the presence of 5 μM of DHA for 48 h compared with that of the untreated cells (data not shown). Thus a 5.0 μM concentration of DHA was selected to test its anti-amyloidogenic toxic effect on SH-SY5Y cells. Fibrillogenesis in the culture media was confirmed by TEM (Fig. 5a), ThT-emission peak (Fig. 5b) and immunoassay with anti-$A\beta_{1-42}$ antibody (Fig. 5d, arrowhead). DHA exhibited significant anti-amyloidogenic toxicity, as indicated by the higher MTT-reduction efficiency, when compared with that of the untreated cells (Fig. 5c). Cells treated with $A\beta_{1-42}$ for 48 h demonstrated altered neuritic sprouting with dystrophic axodendritic systems, while the $A\beta_{1-42}$ + DHA-treated cells

LOW RESOLUTION COLOUR FIG

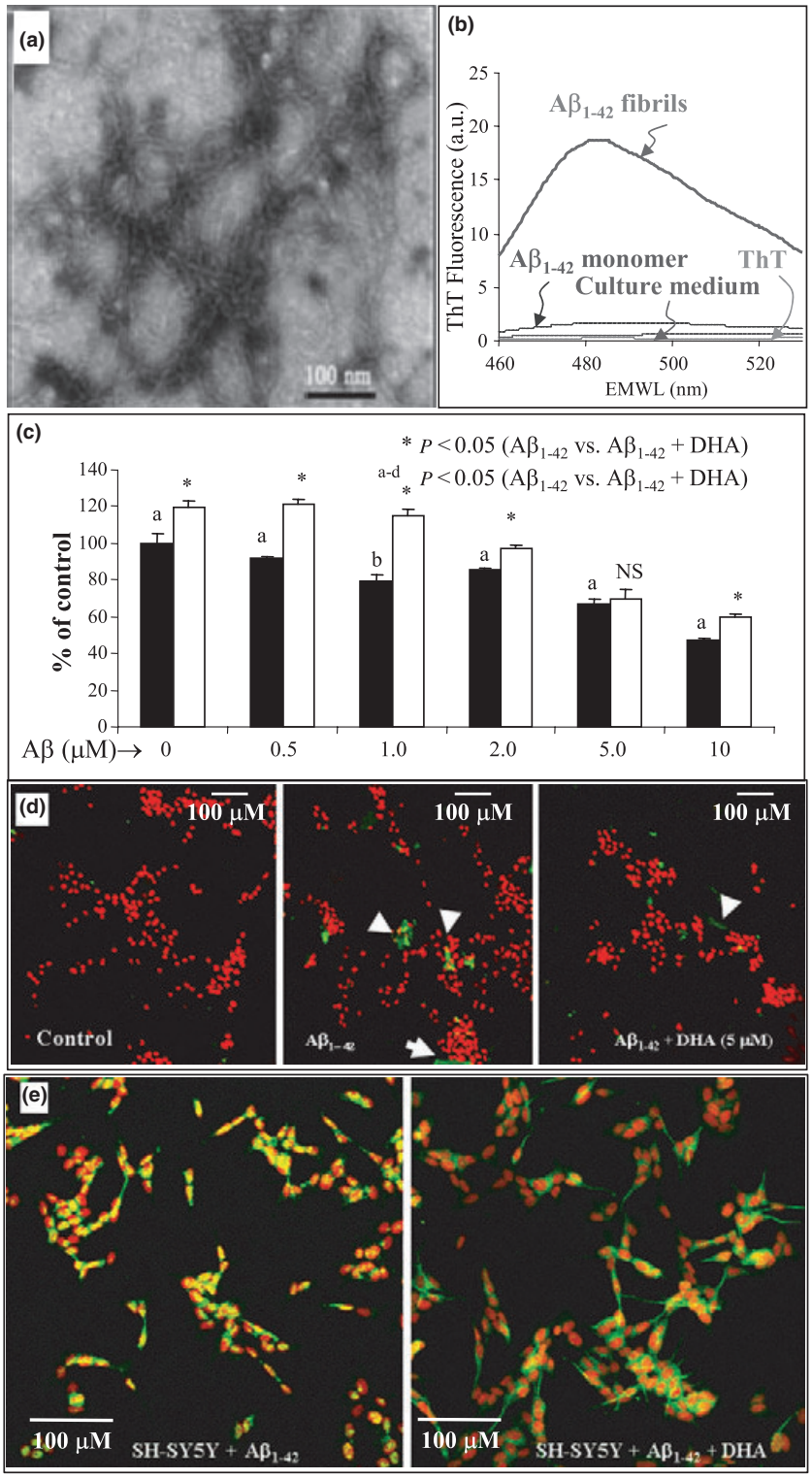

Fig. 5 Neuronally differentiated SH-SY5Y cells were incubated with $A\beta_{1-42}$ in the absence or presence of DHA for 24 h to commence fibrillation in the medium. Fibrillation was confirmed by TEM (a) and ThT-emission peak at 487 nm (b). The anti-amyloidogenic effect of DHA was evaluated by the MTT assay (c). The Aβ deposits, probed with $A\beta_{1-42}$-anti-human Aβ [N] antibody, were seen at or around the cells (arrowheads), and the degree of aggregation was lower in the $A\beta_{1-42}$ + DHA samples (d). The qualitative effect of DHA is shown by representative morphological changes of $A\beta_{1-42}$ and $A\beta_{1-42}$ + DHA-treated cells (e). Altered neuritic sprouting with dystrophic axodendritic systems are clearly observed after the treatment of cells with $A\beta_{1-42}$ for 24 h. DHA inhibited the toxicity, however, as indicated by the appearance of well-defined axodendritic sprouting processes, good viability and full spherical somas (see Materials and methods).

had the appearance of well-defined axodendritic sprouting processes, good viability, including full, spherical somas (Fig. 5e). Thus the *in vitro* inhibitory effect of DHA on fibrillation and the associated toxicity was also evident in the *in vitro* cell culture model.

Discussion

A deficiency of DHA is implicated in AD brains exhibiting fibrillar amyloid deposits. Therefore, the aim of this study was to examine whether DHA inhibits *in vitro* $A\beta_{1-42}$

 J. Neurochem. (2009) 10.1111/j.1471-4159.2009.06336.x

fibrillation and whether such an anti-$A\beta_{1-42}$ outcome affects the neurotoxicity of SH-SY5Y cells, and what the putative mechanism of the action of DHA is. On the basis of the results of quantitative ThT fluorescence assays, qualitative laser microfluorescence analysis and TEM, our study clearly indicates that DHA inhibits *in vitro* fibrillogenesis of $A\beta_{1-42}$, with a concurrent inhibition of $A\beta_{1-42}$-induced toxicity of SH-S5Y5 cells. The inhibitory effect of DHA on fibrillation is dose-dependent and at the tri/tetramer level of $A\beta_{1-42}$ oligomers. Our kinetic data of $A\beta_{1-42}$ fibrillogenesis are consistent with the typical model of fibrillation, which passes through a lag phase, when the Aβ sheets stack to form the nucleus, then through a rapid growth phase to reach a plateau. DHA delayed the lag phase and decelerated the exponential growth of fibrils, demonstrating that DHA inhibits fibrillation by acting during both nucleus formation (oligomerization) and propagation of oligomers (elongation) into mature fibrils. The decreased oligomer levels, as determined by antibody assays, further support the kinetics data indicating that DHA decreases both the formation and stabilization of oligomers and hence their propagation into fibrils.

Investigation of the oligomer size that could have been affected by DHA revealed two bands of an apparent molecular mass ~15 and ~20 kDa. DHA-induced decrease in the density of the two bands indicated that these protofibrillar on-pathway intermediate oligomers were inhibited by DHA. DHA-induced intervention was also evident from the morphology of $A\beta_{1-42}$ fibrils. Some of the $A\beta_{1-42}$ control fibrils, 18 ± 1.25 nm in diameter with a twisting helical pattern, exhibited projections extending from the body. The projections probably act as growing edges for the incoming oligomeric units. Some of the grids of the $A\beta_{1-42}$ controls had protofibrils (beaded chain) composed of spherical oligomers. This has also been found for $A\beta_{1-42}$ at physiological pH (Stine *et al.* 2003). In contrast, TEM grids of the $A\beta_{1-42}$ + DHA samples were almost devoid of fibrils, containing, if at all, only a very small number of fibrils with diffused, shorter and narrower morphology. As DHA kinetically delayed and decelerated fibrillogenesis, the morphological transformation of $A\beta_{1-42}$ might be because of the effect of DHA.

Associations of the C-terminal amino acid R-groups and those of the central hydrophobic core are important determinants for amyloid polymerization (Kirkitadze *et al.* 2001). The quicker fibrillation rate of $A\beta_{1-42}$ is attributed to increased hydrophobicity (Stine *et al.* 2003). Hydrophobicity increases by the mutation of glutamate22 to glutamine in Aβ demonstrating hereditary cerebral hemorrhage with amyloidosis (Dutch type) and leads to a higher rate of fibril formation (Clements *et al.* 1993). To gain insight into DHA-induced inhibition, we focused on intrinsic fluorophore Tyr10 to determine whether its emission intensity is affected by DHA. Bemporad *et al.* (2006) have reported that the presence of aromatic residues, particularly of tyrosine, and phenylalanine plays a major role in molecular recognition, promotes amyloid formation and stabilizes the resulting fibrils. The underlying mechanism includes lateral stacking of the aromatic rings of β sheets (Gazit 2002). Our speculation that Tyr10 in the $A\beta_{1-42}$ backbone is engrossed (or entangled) in a region that acts as a site for intermolecular stacking during fibrillation, is based on the observation that Tyr10 intrinsic emission of $A\beta_{1-42}$ monomers decreases during fibrillation and increases during defibrillation. The emission of Tyr10 depends on a variety of factors including hydrophobicity of the medium, which decreases its fluorescence. The DHA-induced inhibition of $A\beta_{1-42}$ fibrillation further reduced Tyr10 emission, although no shift of the emission maximum was evident, demonstrating that the inhibition perturbs the local environment of Tyr10. We speculate that the 'hexagonal-stacking-of-nucleus' and/or 'beading-to-string' of oligomers is inhibited by hydrophobic DHA from the π-stacking of planar aromatic rings. In so doing, DHA shields Tyr10 into a more hydrophobic pocket that is different from that of the matrix of $A\beta_{1-42}$, and spatially affects its conformation, emission and, consequently, reduces fibrillation. To gain additional insight into DHA-induced inhibition, we evaluated the exposure of Tyr10 to the solvent of $A\beta_{1-42}$ monomers and $A\beta_{1-42}$ fibers in the presence or absence of DHA by determining Tyr10's fluorescence quenching with the use of acrylamide. The K_{sv} values decreased significantly in $A\beta_{1-42}$ fibers, when compared with those of monomeric $A\beta_{1-42}$, indicating decreased exposure of Tyr10 to acrylamide. DHA further decreased the values of K_{sv} in descending order of (20, 10, and 5 μM of DHA), demonstrating a further shielding of Tyr10 into the hydrophobic milieu of DHA. Tyr10 is, therefore, obviously protected by DHA in the $A\beta_{1-42}$ + DHA samples, i.e. it is less accessible to the quencher. The inaccessibility may relate to the interaction between DHA and Tyr10. The interactions between Tyr10 and hydrophobic DHA are, thus, again considered to affect Tyr10 conformation, emission and, hence, fibrillation. If the interaction of Tyr10 with DHA is not hydrophobic by nature, the ionic strength would have some effect on the interaction. To reveal the nature of the interaction, Tyr10 emission quenching was also measured in the presence of gradually increasing concentrations of KI. I^- quenched the emission only slightly (data not shown), indicating that the interaction between DHA and Tyr10 in the assembly buffer was most probably hydrophobic, not electrostatic.

Tyrosine 10 has notable implications in Aβ fibrillation; in particular, Tyr10-gated electrons with a concomitant formation of DT is key to the toxic mechanism of AD Aβ (Barnham *et al.* 2004). The effect of DHA on DT formation is of considerable clinical interest. The levels of DT increased in the $A\beta_{1-42}$ controls, within the limits of our experimental error. DHA significantly reduced the levels of DT in the

$A\beta_{1-42}$ + DHA samples, indicating that DHA-induced inhibition of $A\beta_{1-42}$ fibrillation is, at least partially, related to its anti-DT property. In addition, DHA has a strong anti-order (disordering) property because of its inherent large hydrophobic volume, higher average area per molecule, and spring-like efficacy because of rapid interconversion between extended and bent conformations (Stillwell and Wassall 2003). In contrast, Aβ-fibers are sterically stacked and highly ordered structures. The high anti-order/hydrophobic property of DHA may therefore relate to its anti-fibril properties.

To justify whether the DHA-induced inhibition of fibrillation positively affects the toxicity produced by $A\beta_{1-42}$, we initiated fibrillation directly in the culture medium of SH-SY5Y cells. Fibrillation (Fig. 5a, b, and d) of $A\beta_{1-42}$ evidently occurred in the culture medium with a concurrent production of oligomers. Notably, DHA inhibited the *in vitro* levels of oligomers by restraining their formation. Oligomers have also been detected in the medium of cultured cells (Podlisny *et al.* 1995), indicating that they lie in the 'on-pathway' of fibrillation in the culture medium. Toxicity, as evaluated by MTT-reduction (Fig. 5c) and morphological examinations (Fig. 5e), decreased significantly in the presence of DHA, demonstrating that DHA inhibits *in situ* $A\beta_{1-42}$ fibrillation, and in so doing, reduces the $A\beta_{1-42}$ oligomer-induced toxicity in neuronal cells.

Other studies on fatty acids and fibrillation suggest that fatty acids, at concentrations that favor (lipid)vesicle formation in the assembly buffer, stimulate nucleation and polymerization of α-synuclein (Zhu and Fink 2003) and tau (Gamblin *et al.* 2000). Oleic acid at a concentration of 0.64 mM inhibits amyloid formation at pH 4–5 (Yang *et al.* 2006). Under our experimental conditions, free DHA at > 40 μM, pH 7.4, showed an increased tendency to enhance $A\beta_{1-42}$ fibrillation, suggesting that DHA at high concentrations (> 40 μM) increases oligomer formation by favoring Aβ-nucleation; ethylester-DHA and 1-palmitoyl-2-docosahexaenoyl phosphitidylcholine also increased the fibrillation to an even greater extent (data not shown). Therefore, the presence of DHA either in free or micellar condition in the face of the bulk of the individual amyloid molecules is very critical to affect the fibrillation of $A\beta_{1-42}$. DHA helps in minimizing cognitive loss (Innis 2007). DHA-derived 10, 17-*S*-docosatriene suppresses $A\beta_{1-42}$-induced neurotoxicity (Lukiw *et al.* 2005). Remarkably, DHA cannot be synthesized by neurons but is taken up usually from the extraneural medium after its release from astroglial/cerebral endothelial 12 cells (Moore 2003) and/or phospholipids of these neurovascular cells (Bazan 2008). Thus, free DHA is assumed to interact with the extraneuronally existing Aβs so as to inhibit their polymerization in neurodegenerative diseases such as AD, as is evident from the exogenous uses of DHA in the current experimental paradigms. In conclusion, further studies that need to be conducted for determining whether dietary DHA prevents $A\beta_{1-42}$-induced neurobehavioral deficits in AD model rats, are ongoing in our laboratory. If $A\beta_{1-42}$-oligomers could be inhibited *in vivo*, as they are *in vitro*, DHA would be an worthy therapeutic agent against $A\beta_{1-42}$-induced AD. In particular, as DHA is an essential brain nutrient and can easily cross the blood–brain barrier, the risk from its cytotoxic side effects would be minimal.

Acknowledgements

The authors acknowledge the help of Tsunao Yoneyama, technician Shimane University Faculty of Medicine in TEM studies. This work was supported in part by a grant-in-Aid for Scientific Research from the Ministry of Education, Science and Culture of Japan (19500324 to MH).

References

Atwood C. S., Perry G., Zeng H. *et al.* (2004) Copper mediates dityrosine cross-linking of Alzheimer's amyloid-β. *Biochemistry* **43**, 560–568.

Barnham K. J., Haeffner F., Ciccotosto G. D. *et al.* (2004) Tyrosine gated electron transfer is key to the toxic mechanism of Alzheimer's disease β-amyloid. *FASEB J.* **18**, 1427–1429.

Bazan N. G. (2008) Neuroprotectin D1-mediated anti-inflammatory and survival signaling in stroke, retinal degenerations and Alzheimer's disease. *J. Lipid Res.*; DOI: 10.1194/jlr.R800068-JLR200. 13

Bemporad F., Taddei N., Stefani M. and Chiti F. (2006) Assessing the role of aromatic residues in the amyloid aggregation of human muscle acylphosphatase. *Protein Sci.* **15**, 862–870.

Berman D. E., Dall'Armi C., Voronov S. V., McIntire L. B., Zhang H., Moore A. Z., Staniszewski A., Arancio O., Kim T. W. and Di Paolo G. (2008) Oligomeric amyloid-β peptide disrupts phosphatidylinositol-4,5-bisphosphate metabolism. *Nat. Neurosci.* **11**, 547–554.

Bitan G., Kirkitadze M. D., Lomakin A., Vollers S. S., Benedek G. B. and Teplow D. B. (2003) Amyloid β-protein (Aβ) assembly: Aβ40 and Aβ42 oligomerize through distinct pathways. *Proc. Natl Acad. Sci. USA* **100**, 330–335.

Burdick D., Soreghan B., Kwon M., Kosmoski J., Knauer M., Henschen A., Yates J., Cotman C. and Glabe C. (1992) Assembly and aggregation properties of synthetic Alzheimer's A4/β amyloid peptide analogs. *J. Biol. Chem.* **267**, 546–554.

Clements A., Walsh D. M., Williams C. H. and Allsop D. (1993) Effects of the mutations Glu22 to Gln and Ala21 to Gly on the aggregation of a synthetic fragment of the Alzheimer's amyloid β/A4 peptide. *Neurosci. Lett.* **161**, 17–20.

Fraser P. E., Nguyen J. T., Surewicz W. K. and Kirschner D. A. (1991) pH-dependent structural transitions of Alzheimer's amyloid peptides. *Biophys. J.* **60**, 1190–1201.

Gamblin T. C., King M. E., Kuret J., Berry R. W. and Binder L. I. (2000) Oxidative regulation of fatty acid induced tau polymerization. *Biochemistry* **39**, 14203–14210.

Gazit E. (2002) A possible role for π-stacking in the self-assembly of amyloid fibrils. *FASEB J.* **6**, 77–83.

Glabe C. G. (2004) Conformation-dependent antibodies target diseases of protein misfolding. *Trends Biochem. Sci.* **29**, 542–547.

Haass C. and Selko D. J. (2007) Soluble protein oligomers in neurodegeneration: lessons from the Alzheimer's amyloid β-peptide. *Nat. Rev. Mol. Cell Biol.* **8**, 101–112.

Hashimoto M., Hossain S., Shimada T., Sugioka K., Yamasaki H., Fujii Y., Ishibashi Y., Oka J. and Shido O. (2002) Docosahexaenoic acid provides protection from impairment of learning

ability in Alzheimer's disease model rats. *J. Neurochem.* **81**, 1084–1091.

Hashimoto M., Hossain S. and Shido O. (2005a) Docosahexaenoic acid-induced amelioration on impairment of memory learning in amyloid β-infused rats relates to the decreases of amyloid β and cholesterol levels in detergent-insoluble membrane fractions. *Biochim. Biophys. Acta* **1738**, 91–98.

Hashimoto M., Tanabe Y., Fujii Y., Kikuta T., Shibata H. and Shido O. (2005b) Chronic administration of docosahexaenoic acid ameliorates the impairment of spatial cognition learning ability in amyloid β-infused rats. *J. Nutr.* **135**, 549–555.

Hashimoto M., Shahdat H. M., Yamashita S. *et al.* (2008) Docosahexaenoic acid disrupts in vitro amyloid β fibrillation and concomitantly inhibits amyloid levels in cerebral cortex of Alzheimer's disease model rats. *J. Neurochem.* **107**, 1634–1646.

Innis S. M. (2007) Dietary (n-3) fatty acids and brain development. *J. Nutr.* **137**, 855–859.

Iwatsubo T., Odaka A., Suzuki N., Mizusawa H., Nukina N. and Ihara Y. (1994) Visualization of Aβ 42(43) and Aβ 40 in senile plaques with end-specific Aβ monoclonals: evidence that an initially deposited species is Aβ 42(43). *Neuron* **13**, 45–53.

Jarrett J. T., Berger E. P. and Lansbury P. T. Jr (1993) The carboxy terminus of the β amyloid protein is critical for the seeding of amyloid formation: implications for the pathogenesis of Alzheimer's disease. *Biochemistry* **32**, 4693–4697.

Kato Y., Maruyama W., Naoi M., Hashizume Y. and Osawa T. (1998) Immunohistochemical detection of dityrosine in lipofuscin pigments in the aged human brain. *FEBS Lett.* **439**, 231–234.

Kayed R., Head E., Thompson J. L., McIntire T. M., Milton S. C., Cotman C. W. and Glabe C. G. (2003) Common structure of soluble amyloid oligomers implies common mechanism of pathogenesis. *Science* **300**, 486–489.

Kirkitadze M. D., Condron M. M. and Teplow D. B. (2001) Identification and characterization of key kinetic intermediates in amyloid β-protein fibrillogenesis. *J. Mol. Biol.* **312**, 1103–1119.

Lim G. P., Calon F., Morihara T., Yang F., Teter B., Ubeda O., Salem Jr N., Frautschy S. A. and Cole G. M. (2005) A diet enriched with the omega-3 fatty acid docosahexaenoic acid reduces amyloid burden in an aged Alzheimer's mouse model. *J. Neurosci.* **25**, 3032–3040.

Lukiw W. J., Cui J. G., Victor L., Marcheselli V. L., Bodker M., Botkjaer A., Gotlinger K., Serhan C. N. and Bazan N. G. (2005) A role for docosahexaenoic acid-derived neuroprotectin D1 in neural cell survival and Alzheimer's disease. *J. Clin. Invest.* **115**, 2774–2783.

Ma Z. and Westermark G. T. (2002) Effects of free fatty acid on polymerization of islet amyloid polypeptide (IAPP) in vitro and on amyloid fibril formation in cultivated isolated islets of transgenic mice overexpressing human IAPP. *Mol. Med.* **8**, 863–868.

Moore S. A. (2003) Polyunsaturated fatty acid synthesis and release by brain-derived cells in vitro. *J. Mol. Neurosci.* **16**, 195–200.

Morris M. C., Evans D. A., Bienias J. L., Tangney C. C., Bennett D. A., Wilson R. S., Aggarwal N. and Schneider J. (2003) Consumption of fish and n-3 fatty acids and risk of incident Alzheimer's disease. *Arch. Neurol.* **60**, 940–946.

Padrick S. B. and Miranker A. D. (2001) Islet amyloid polypeptide: identification of long-range contacts and local order on the fibrillogenesis pathway. *J. Mol. Biol.* **308**, 783–794.

Podlisny M. B., Ostaszewski B. L., Squazzo S. L., Koo E. H., Rydell R. E., Teplow D. B. and Selkoe D. J. (1995) Aggregation of secreted amyloid-protein into sodium dodecyl sulfate-stable oligomers in cell culture. *J. Biol. Chem.* **270**, 9564–9570.

Prasad M. R., Lovell M. A., Yatin M., Dhillon H. and Markesbery W. R. (1998) Regional membrane phospholipid alterations in Alzheimer's disease. *Neurochem. Res.* **23**, 81–88.

Selkoe D. J. (1991) The molecular pathology of Alzheimer's disease. *Neuron* **6**, 487–498.

Serpell L. C. (2000) Alzheimer's amyloid fibrils: structure and assembly. *Biochim. Biophys. Acta Mol. Basis. Dis.* **1502**, 16–30.

Söderberg M., Edlund C., Kristensson K. and Dallner G. (1991) Fatty acid composition of brain phospholipids in aging and in Alzheimer's disease. *Lipids* **26**, 421–425.

Stillwell W. and Wassall S. R. (2003) Docosahexaenoic acid: membrane properties of a unique fatty acid. *Chem. Phys. Lipids* **126**, 1–27.

Stine W. B., Dahlgren K. N., Krafft G. A. and LaDu M. J. (2003) In vitro characterization of conditions for amyloid-β peptide oligomerization and fibrillogenesis. *J. Biol. Chem.* **278**, 11612–11622.

Yang F., Zhang M., Zhou B. R., Chen J. and Liang Y. (2006) Oleic acid inhibits amyloid formation of the intermediate of α-lactalbumin at moderately acidic pH. *J. Mol. Biol.* **362**, 821–834.

Zhu M. and Fink A. L. (2003) Lipid binding inhibits α-synuclein fibril formation. *J. Biol. Chem.* **278**, 16873–16877.

Author Query Form

Journal: JNC

Article: 6336

Dear Author,
During the copy-editing of your paper, the following queries arose. Please respond to these by marking up your proofs with the necessary changes/additions. Please write your answers on the query sheet if there is insufficient space on the page proofs. Please write clearly and follow the conventions shown on the attached corrections sheet. If returning the proof by fax do not write too close to the paper's edge. Please remember that illegible mark-ups may delay publication.

Many thanks for your assistance.

Query reference	Query	Remarks
1	**AUTHOR: Please check the cell line – SH-SY5Y or SH-S5Y5. Both of them are used. Please confirm which one(or both) is correct.**	
2	**AUTHOR: Please give address information for 'Biosource International, Inc.': town or city.**	
3	**AUTHOR: Please give address information for 'Cayman Chemical Company': town or city.**	
4	**AUTHOR: Please give address information for 'Hitachi': town/city, state, and country.**	
5	**AUTHOR: Please give manufacturer information for 'I**MAGE**J**': company name, town, state (if USA), and country.	
6	**AUTHOR: Please provide the appropriate section heading in place of the text 'as described below'.**	
7	**AUTHOR: As per journal style, TBST mentioned less than three times in the article are expanded in full. If expansion incorrect please insert correct expansion.**	
8	**AUTHOR: Glabes, 1984 has been changed to Glabe 2004 so that this citation matches the Reference List. Please confirm that this is correct.**	
9	**AUTHOR: Please give address information for 'Amersham, GE Health Care': town/city, state, and country.**	
10	**AUTHOR: It is journal style for abbreviations, which are used less than three times to be fully spelled out. Please define abbreviation PLSD here in the text.**	
11	**AUTHOR: Does this 'KI' refers to potassium iodide? Please check.**	
12	**AUTHOR: Moore, 2001 has been changed to Moore 2003 so that this citation matches the Reference List. Please confirm that this is correct.**	

13	**AUTHOR: Please provide the volume number and page range for reference Bazan (2008).**	
14	**AUTHOR: Ma and Westermark (2002) has not been cited in the text. Please indicate where it should be cited; or delete from the Reference List.**	
15	**AUTHOR: Figure 1 has been saved at a low resolution of 156 dpi. Please resupply at 600 dpi. Check required artwork specifications at http:// www.blackwellpublishing.com/authors/digill.asp**	
16	**AUTHOR: Figure 2 has been saved at a low resolution of 251 dpi. Please resupply at 600 dpi. Check required artwork specifications at http:// www.blackwellpublishing.com/authors/digill.asp**	
17	**AUTHOR: Figure 3 has been saved at a low resolution of 109 dpi. Please resupply at 600 dpi. Check required artwork specifications at http:// www.blackwellpublishing.com/authors/digill.asp**	
18	**AUTHOR: Figure 4 has been saved at a low resolution of 177 dpi. Please resupply at 600 dpi. Check required artwork specifications at http:// www.blackwellpublishing.com/authors/digill.asp**	
19	**AUTHOR: Figure 5 has been saved at a low resolution of 106 dpi. Please resupply at 600 dpi. Check required artwork specifications at http:// www.blackwellpublishing.com/authors/digill.asp**	

USING E-ANNOTATION TOOLS FOR ELECTRONIC PROOF CORRECTION

Required Software

Adobe Acrobat Professional or Acrobat Reader (version 7.0 or above) is required to e-annotate PDFs. Acrobat 8 Reader is a free download: http://www.adobe.com/products/acrobat/readstep2.html

Once you have Acrobat Reader 8 on your PC and open the proof, you will see the Commenting Toolbar (if it does not appear automatically go to Tools>Commenting>Commenting Toolbar). The Commenting Toolbar looks like this:

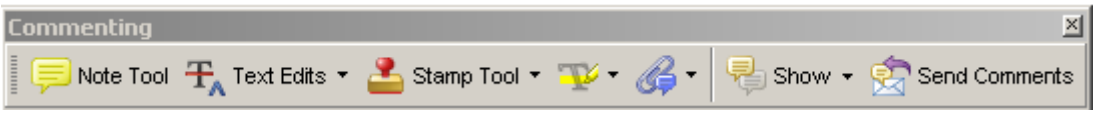

If you experience problems annotating files in Adobe Acrobat Reader 9 then you may need to change a preference setting in order to edit.

In the "Documents" category under "Edit – Preferences", please select the category 'Documents' and change the setting "PDF/A mode:" to "Never".

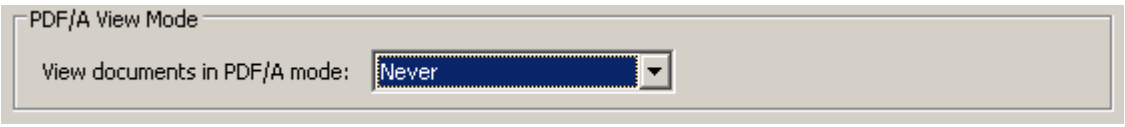

Note Tool — For making notes at specific points in the text

Marks a point on the paper where a note or question needs to be addressed.

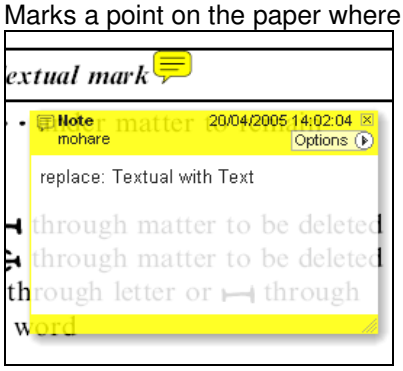

How to use it:

1. Right click into area of either inserted text or relevance to note
2. Select Add Note and a yellow speech bubble symbol and text box will appear
3. Type comment into the text box
4. Click the X in the top right hand corner of the note box to close.

Replacement text tool — For deleting one word/section of text and replacing it

Strikes red line through text and opens up a replacement text box.

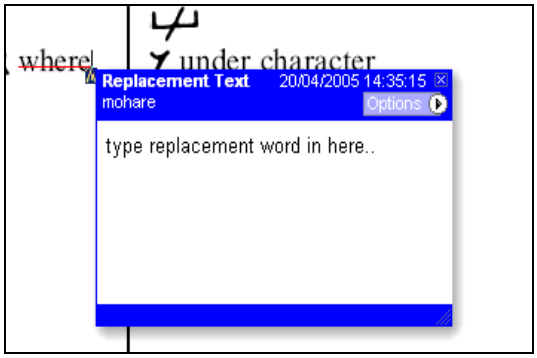

How to use it:

1. Select cursor from toolbar
2. Highlight word or sentence
3. Right click
4. Select Replace Text (Comment) option
5. Type replacement text in blue box
6. Click outside of the blue box to close

Cross out text tool — For deleting text when there is nothing to replace selection

Strikes through text in a red line.

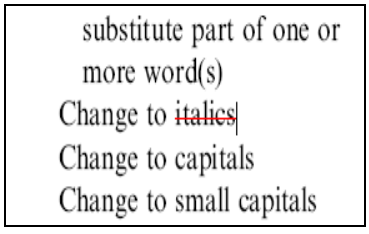

How to use it:

1. Select cursor from toolbar
2. Highlight word or sentence
3. Right click
4. Select Cross Out Text

Approved tool — For approving a proof and that no corrections at all are required.

How to use it:

1. Click on the Stamp Tool in the toolbar
2. Select the Approved rubber stamp from the 'standard business' selection
3. Click on the text where you want to rubber stamp to appear (usually first page)

Highlight tool — For highlighting selection that should be changed to bold or italic.

Highlights text in yellow and opens up a text box.

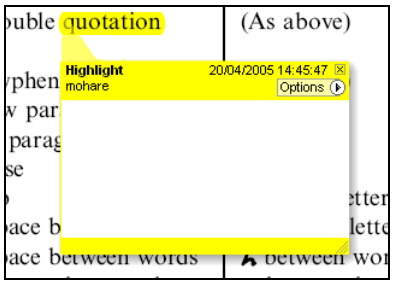

How to use it:

1. Select Highlighter Tool from the commenting toolbar
2. Highlight the desired text
3. Add a note detailing the required change

Attach File Tool — For inserting large amounts of text or replacement figures as a files.

Inserts symbol and speech bubble where a file has been inserted.

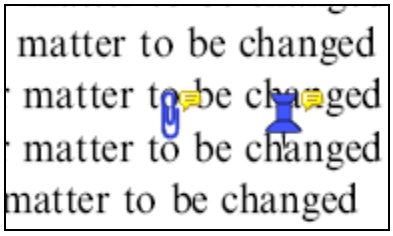

How to use it:

1. Click on paperclip icon in the commenting toolbar
2. Click where you want to insert the attachment
3. Select the saved file from your PC/network
4. Select appearance of icon (paperclip, graph, attachment or tag) and close

Pencil tool — For circling parts of figures or making freeform marks

Creates freeform shapes with a pencil tool. Particularly with graphics within the proof it may be useful to use the Drawing Markups toolbar. These tools allow you to draw circles, lines and comment on these marks.

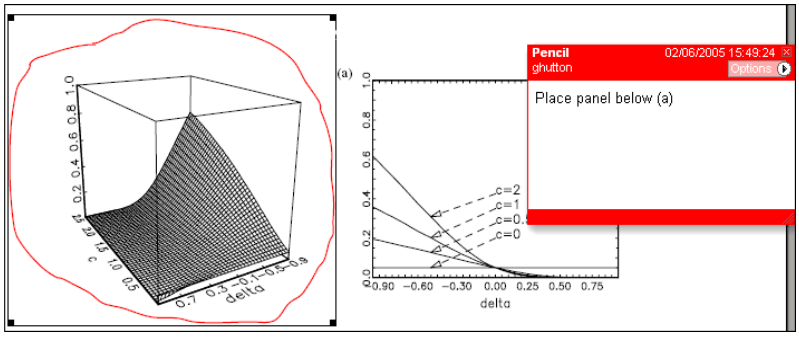

How to use it:

1. Select Tools > Drawing Markups > Pencil Tool
2. Draw with the cursor
3. Multiple pieces of pencil annotation can be grouped together
4. Once finished, move the cursor over the shape until an arrowhead appears and right click
5. Select Open Pop-Up Note and type in a details of required change
6. Click the X in the top right hand corner of the note box to close.

Help

For further information on how to annotate proofs click on the Help button to activate a list of instructions: